Object Gathering with a Tethered Robot Duo

Yao Su[1] Yuhong Jiang[1] Yixin Zhu[1,2] Hangxin Liu[1]

***Abstract*—We devise a cooperative planning framework to generate optimal trajectories for a robot duo tethered by a flexible net to gather scattered objects spread in a large area. Specifically, the proposed planning framework first produces a set of dense waypoints for each robot, serving as the initialization for optimization. Next, we formulate an iterative optimization scheme to generate smooth and collision-free trajectories while ensuring cooperation within the robot duo to gather objects efficiently and avoid obstacles properly. We validate the generated trajectories in simulation and implement them in physical robots using Model Reference Adaptive Control (MRAC) to handle unknown dynamics of carried payloads. In a series of studies, we find that: (i) a U-shape cost function for maintaining separation distance is effective in planning cooperative robot duo, and (ii) the task efficiency is not always proportional to the tethered net's length. Given an environment configuration, our framework can gauge the optimal net length. To our best knowledge, ours is the first that provides such estimation for tethered robot duo.**

***Index Terms*—Cooperative path planning, optimization, tethered WMRs, adaptive control.**

I. Introduction

WE consider the task of gathering and carrying objects scattered on the floor by deploying two Wheeled Mobile Robots (WMRs) tethered by a flexible net or rope as a duo. Compared to picking and placing individual objects one by one, this setting is more intriguing and compelling for robots to collect small items spread across a large area autonomously. Fig. 1a showcases two similar tasks in the physical world that share a similar spirit, wherein humans adopt a net to collect scattered objects with high efficiency.

The tethered robot duo must resolve two challenges. First, how to effectively generate **cooperative** trajectories spanned between two individuals? Despite a robot duo could accomplish more complex and dexterous tasks than a single robot [1], the physical connection among it also introduces additional constraints in planning. Compared with prior work concerning rigid connections (*e.g.*, [2, 3]), planning for the robot duo with a non-rigid connection (*e.g.*, a rope or a net) is more challenging [4, 5]; one has to consider the task goals, obstacle avoidance, and net shape maintenance through individual's behaviors. Second, the tethered robot duo is subjected to **increasing payloads** during operation. In addition to the friction force introduced by the net, the dragging force increases significantly and deteriorates the trajectory tracking of each robot as the task progresses and more objects are gathered. Of note, this challenge is mostly overlooked in literature [4–7].

Manuscript received: September 9, 2021; Revised: November 25, 2021; Accepted: December 22, 2021. This paper was recommended for publication by Editor Lucia Pallottino upon evaluation of the Associate Editor and Reviewers' comments. (*Corresponding author: Hangxin Liu*)

[1] Beijing Institute for General Artificial Intelligence (BIGAI).
[2] Institute for Artificial Intelligence, Peking University.
Emails: {suyao, jiangyuhong, y, liuhx}@bigai.ai

Digital Object Identifier (DOI): see top of this page.

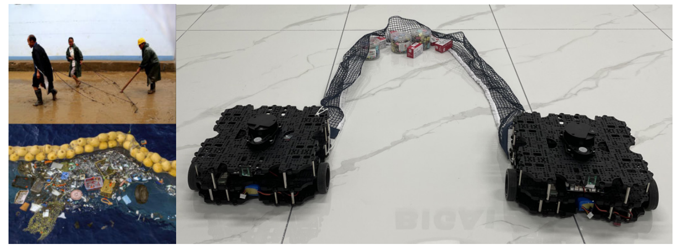

(a) (b)

Fig. 1: (a) **Two examples in daily life.** Humans use long/flexible structures to gather scattered objects, a similar setup akin to the one proposed in our work (Source: online). (b) **Two Wheeled Mobile Robots (WMRs) tethered by a net as a duo.** Our framework **cooperatively** plans the robot duo's trajectories, indirectly maintaining the net's shape through motions. It also handles the **uncertainty** of the increasing payloads using Model Reference Adaptive Control (MRAC) to properly track the trajectories during operation.

In this paper, we devise an optimization-based cooperation framework for a pair of tethered WMRs (*i.e.*, a duo) to gather and transport objects with a net; see Fig. 1b for the setup. The core of our framework is a trajectory optimization scheme that produces smooth trajectories for the robot duo, which jointly accounts for task goals, obstacle avoidance, and net shape maintenance. A set of waypoints extended from a centerline connecting all the target objects along the robots' initial and final configurations serve as the initialization for the optimization scheme. An MRAC controller is further implemented to track the produced trajectories under unknown increasing payloads stably. Our framework is validated in both simulation and experiment.

A. Related Work

Although **cooperative planning** has incubated many successful applications, such as search and rescue [8], exploration [9], object manipulation [10, 11], payload transportation [12, 13], the planning problem of tethered robot duo to date is less explored. Prior work [4, 14] mostly formulates it as a separation problem: The goal is to find trajectories for the robot duo to separate all target objects from obstacles. In such a scheme, prior methods assume an infinite separation distance between the robots, unpractical and unrealistic in many cases. Although Teshnizi *et al*. [5] relax this assumption and introduce a modified A* planning algorithm given specific tether lengths, it fails to properly account for the obstacle avoidance (*e.g.*, in final configuration) and net shape maintenance. We fully address these challenges in a new framework.

Gathering objects using the robot duo necessitates maintaining the shape of the flexible tether connecting the robots, though not necessarily precisely. Several setups have showcased the ability to **handle flexible connections** in diverse scenarios among robots. For instance, a dual-arm robot manipulates rope-like objects in clutter [15], three quadcopters connected by a net catch and throw a ball [11], multiple robots manipulate deformable bed sheet [16], a visual servoing scheme maintains the tether's shape between two-wheel robots [17, 18], and a pair of tethered quadcopters move an object using the tether [6, 7]. Although the above literature strongly suggests the significance of maintaining tether/net shapes in cooperative planning, directly and precisely controlling its shape is oftentimes unnecessary, resulting in increased complexity in both modeling and control. To tackle this problem, our proposed framework adopts a U-shape cost function to maintain a proper distance between the two tethered robots, such that the net shape is indirectly controlled.

As an essential branch of robust control, **Model Reference Adaptive Control (MRAC)** can maintain the platform's stability with unmodeled dynamics. It has been implemented on various robot platforms with inaccurate physical parameters, unknown payloads, or external disturbance [19]. For example, a tilt-rotor quadcopter platform using MRAC pulls an unmodeled cart [20], and WMRs adopts MRAC maintain the platform stability with inaccurate physical parameters [21]. Similarly, we implement MRAC on the tethered robot duo for the object gathering task, since the physical parameters of the objects are unknown, and the drag force increases with more objects collected by the net.

B. Overview

We organize the remainder of the paper as follows. Section II presents the proposed cooperative path planning framework for the tethered robot duo. Section III describes the implementation of MRAC on the robot duo for robust trajectory tracking. Section IV and Section V show the simulation and experiment results with comprehensive evaluations, respectively. We conclude the paper in Section VI.

II. Cooperative Path Planning

This section formally describes the proposed cooperative path planning framework for the tethered robot duo, assuming the environment and object locations are known.

A. Problem Setup

Fig. 2 illustrates our problem setup. Given an environment with a set of objects (red squares) and obstacles (black blocks), a robot duo is tasked to navigate from the initial configuration $P_s = (P_s^1, P_s^2)$ to reach the end configuration $P_e = (P_e^1, P_e^2)$ while collecting the objects on-the-way and avoiding obstacles. The environment is described as an occupancy grid Map, wherein $Map(i,j) = 0$, 1, and 2 denote empty grids, grids occupied by obstacles, and grids occupied by objects, respectively. A safety margin γ defined based on the robot's dimension is further added to obstacles for collision

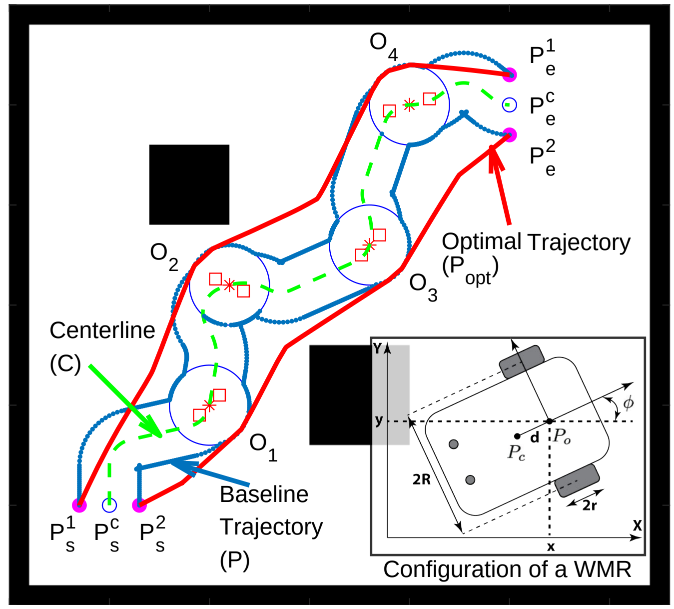

Fig. 2: **The proposed cooperative path planning framework for tethered robot duo.** Our framework generates a centerline C to connect start point P_s^c, end point P_e^c, and all object points, together with a set of waypoints (*i.e.*, baseline trajectory P), who serve as the initialization for the subsequent trajectory optimization to find P_{opt}.

avoidance and to the radius of each target object's minimum bounding circle for safety. We also merge the circles that are closely overlapped. As a result, we have M circles in total $O = \{O_1, \ldots, O_M\}$, where $O_i = [x_i^o, y_i^o, r_i^o]$ includes the center position and radius of each circle. Of note, avoiding obstacles not only requires the robot duo to avoid directly colliding with the obstacle but further demands the tethered net not to enclose any obstacle at any moment.

We devise a two-stage cooperative path planning framework to generate an optimal trajectory, shown also in Fig. 2. First, our framework generates a set of waypoints (blue dots) from the centerline path (dashed green line) that connects the robots' start and end configurations along with the circles that enclose target objects. We call these waypoints *baseline trajectory*; they serve as a good initialization for the subsequent step. Next, our framework performs *trajectory optimization* to produce feasible trajectories (solid red line).

Assumption: Our framework has two assumptions: (i) The circles do not overlap with obstacles; namely, the objects cannot be too close to the obstacle such that the robot duo fails to navigate without violating the safety margin. (ii) The size of the circles is smaller than the length of the tethered net; the net constrains the robot duo's motions.

B. Baseline Trajectory

Let the middle point of the tethered robot duo at the start configuration be $P_s^c = \frac{1}{2}(P_s^1 + P_s^2)$ and at the end configuration be $P_e^c = \frac{1}{2}(P_e^1 + P_e^2)$. First, we adopt a conventional path planning algorithm (hybrid A^* [22] or RRT^* [23]) to construct the centerline by connecting P_s^c, each circle's center point O_i, and P_e^c; see dashed green line in Fig. 2. Formally, the centerline is denoted as $C = \{P_s^c, \ldots, P_e^c\} \in \mathbb{R}^{N\times 3}$,

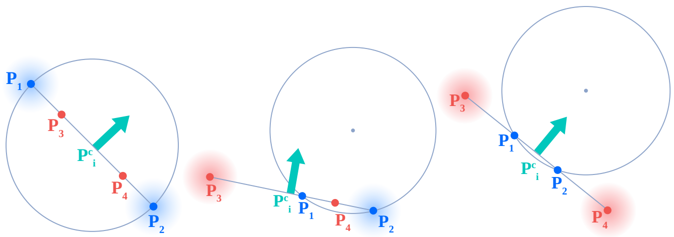

(a) Case 1 (b) Case 2 (c) Case 3

Fig. 3: **The selection of baseline points.** Given the centerline point P_i^c (green arrow), four candidates of baseline points are proposed; Eqs. (2) and (3) yield P_1, P_2 (blue dots), and Eq. (1) yields P_3, P_4 (red dots). Shaded points indicate the selected baseline points P_i^l, P_i^r.

$P_i^c = [x_i^c, y_i^c, \phi_i^c]$, where N is the total number of points. Next, we expand this centerline to form robot duo's baseline trajectories, $P = [P^l, P^r] \in \mathbb{R}^{N\times 6}$; see blue curves in Fig. 2.

Specifically, we divide C into two groups: on or near the circumference of circles C_{circle} and others C_{free}. For point $P_i^c \in C_{\text{free}}$, the baseline trajectory points are given by

$$P_i^l, P_i^r = \begin{bmatrix} x_i^c \pm l\cos(\phi_i^c + \frac{\pi}{2}) \\ y_i^c \pm l\sin(\phi_i^c + \frac{\pi}{2}) \\ \phi_i^c \end{bmatrix}^T, \tag{1}$$

where l is the separation distance chosen based on the dimension of the WMRs. For point $P_i^c \in C_{\text{circle}}$, we first calculate the line in the direction perpendicular to its orientation ϕ_i^c with

$$y = kx + b, \tag{2}$$

where $k = tan(\phi_i^c + \frac{\pi}{2})$, and $b = y_i^c - kx_i^c$. Next, we solve two intersection points, P_1 and P_2, by combining Eq. (2) with the related circle equation of O_j,

$$(x - x_j^o)^2 + (y - y_j^o)^2 = {r_j^o}^2. \tag{3}$$

Another two points obtained by Eq. (1) are denoted as P_3 and P_4. We choose P_i^l, P_i^r from these four candidates by selecting the two outer ones, as shown in Fig. 3.

C. Trajectory Optimization

With the estimated baseline trajectory in Section II-B as the initialization, we further devise an iterative optimization framework to find the optimal trajectory for the tethered duo. Compared with optimizing the whole trajectory at once, our iterative optimization framework improves computational efficiency and avoids local minimum [24, 25]. At each iteration, the trajectory of one mobile robot, denoted as P^1, is optimized, whereas the trajectory of the other robot, denoted as P^2, is treated as a known constant. Algorithm 1 summarizes this framework, where *opt* stands for the nonlinear optimization solver with defined cost functions and constraints.

1) Cost Functions:

Obstacle Cost: We define obstacle cost in two forms: the cost of physical obstacles and the cost of objects as obstacles. The cost of physical obstacles is defined as

$$J_{\text{obs},1}(i) = \begin{cases} K_1, & Map(P^1(i,1), P^1(i,2)) \geqslant 1 \\ 0, & Else \end{cases}, \tag{4}$$

where K_1 is a positive parameter to be selected.

The cost of objects as obstacles treats circles O_j as obstacles, designed similarly to potential field methods [26]:

$$J_{\text{obs},2}(i,j) = \begin{cases} \frac{1}{2}K_2(\frac{1}{D(i,j)} - \frac{1}{r_j^o})^2, & D(i,j) \leqslant r_j^o \\ 0, & D(i,j) > r_j^o \end{cases}, \tag{5}$$

where $D(i,j)$ denotes the Euclidean distance between the trajectory point P_i^1 and the object circle center O_j, and K_2 is a positive parameter to penalize the distance.

As such, the combined obstacle cost of P_i^1 is defined as

$$J_{\text{obs}}(i) = J_{\text{obs},1}(i) + \sum_{j=1}^{M} J_{\text{obs},2}(i,j). \tag{6}$$

Distance Cost: The distance cost is calculated as the weighted sum of the Euclidean distance between two consecutive points and the orientation difference:

$$\begin{aligned} J_{\text{dist}}(i) &= t_1\sqrt{\Delta x_i^2 + \Delta y_i^2} + t_2|\Delta\phi_i|, \\ \Delta x_i &= P^1(i,1) - P^1(i+1,1), \\ \Delta y_i &= P^1(i,2) - P^1(i+1,2), \\ \Delta \phi_i &= P^1(i,3) - P^1(i+1,3), \end{aligned} \tag{7}$$

where t_1 and t_2 are two non-negative parameters.

Expansion Cost: The cost function for expansion is designed as a U-shape cost function [27]:

$$J_e(i) = \begin{cases} k_{d1}\tan^2(\gamma_1 d + \gamma_2), & d_{\min} \leqslant d \leqslant d_{\text{rest}} \\ k_{d2}(d - d_{\text{rest}})^2 - \frac{(d-d_{\text{rest}})^2}{(d-d_{\max})^2}, & d_{\text{rest}} < d \leqslant d_{\max} \\ K_3, & d < d_{\min} \text{ or } d > d_{\max} \end{cases} \tag{8}$$

where $\gamma_1 = \frac{\pi}{2(d_{\text{rest}} - d_{\min})}$, and $\gamma_2 = -\gamma_1 d_{\text{rest}}$. d is the Euclidean distance between trajectory points P_i^1 and P_i^2, representing the expansion of the tethered net. k_{d1}, k_{d2}, and K_3 are gain parameters. $d_{\max}$, $d_{\min}$, and d_{rest} denote the minimum, maximum, and the ideal expansion of the tethered net, set based on various hardware setup and task scenarios.

The reason for having this expansion cost is to maintain the U-shape of the tethered net. Conversely, the net shape would make it infeasible to collect objects when the two WMRs are too close or too far. In this paper, we set $d_{\min} = 0.1 d_{\max}$ and $d_{\text{rest}} = \frac{2}{\pi} d_{\max}$—a half-circle shape. Of note, if $d_{\max}$ is not specified, we can treat it as a random variable to estimate the optimal net length in certain task scenarios.

Smoothness Cost: The smoothness cost is defined as the sum of squared accelerations along the trajectory:

$$J_s = \sum_{j=1}^{3} b_j P^1(:,j)^T Q P^1(:,j), \tag{9}$$

where $Q = A^T A$, and A is the finite difference matrix [28], b_js are weighting gains.

Taken together, the total cost along the whole trajectory is defined by the sum of the above cost functions:

$$J_{\text{total}} = a_1 J_s + \sum_{i=1}^{N} a_2 J_{\text{dist}}(i) + a_3 J_{\text{obs}}(i) + a_4 J_e(i) \tag{10}$$

where a_1, a_2, a_3, and a_4 are weighting gains for costs.

Algorithm 1: Trajectory Optimization Algorithm

Data: $N_{\text{total}}, P, O, Map, t_{1-2}, K_{1-3}, k_{d1}, k_{d2}$
$Q, b_{1-3}, a_{1-4}, \Delta L_{\max}, \Delta\phi_{\max}$
Result: $P_{opt}, d_{\max}$
$step \leftarrow 1, d_{\max} \leftarrow N\Delta L_{\max}$; `// Initialization`
while $step \leqslant N_{total}$ **do**
  if $mod(step, 2) = 1$ **then** `// Optimize left half`
    $P_s \leftarrow P(1, 1:3), P_e \leftarrow P(N, 1:3)$;
    `// Specify start and end points`
    $P^1_{ini} \leftarrow P(2:N\text{-}1, 1:3)$;
    `// Traj to be optimized`
    $P^2_{ini} \leftarrow P(2:N\text{-}1, 4:6)$;
    `// Traj of another half as constant`
    $[P^1_{opt}, d_{\max}] \leftarrow opt(P^1_{ini}, P^2_{ini}, P_s, P_e, Map, O, d_{\max})$;
    `// Optimization process`
    $P(2:N\text{-}1, 1:3) \leftarrow P^1_{opt}$;
    `// Update left half trajectory`
  else `// Optimize right half`
    $P_s \leftarrow P(1, 4:6), P_e \leftarrow P(N, 4:6)$;
    $P^1_{ini} \leftarrow P(2:N\text{-}1, 4:6)$;
    $P^2_{ini} \leftarrow P(2:N\text{-}1, 1:3)$;
    $[P^2_{opt}, d_{\max}] \leftarrow opt(P^1_{ini}, P^2_{ini}, P_s, P_e, Map, O, d_{\max})$;
    $P(2:N\text{-}1, 4:6) \leftarrow P^2_{opt}$;
  end
  $step \leftarrow step + 1$; `// Update steps`
end
$P_{opt} \leftarrow P$; `// Output optimized trajectory`

2) Constraints:

Maximum Velocity Constraint: We define it as:

$$\begin{aligned} 0 \leqslant \sqrt{\Delta x_i^2 + \Delta y_i^2} &\leqslant \Delta L_{\max}, \\ -\Delta\phi_{\max} \leqslant \Delta\phi_i &\leqslant \Delta\phi_{\max}, \end{aligned} \tag{11}$$

where $\Delta L_{\max}$ is the maximum travel distance at each step, and $\Delta\phi_{\max}$ is the maximum turn angle at each step.

Object and Obstacle Constraint: We select consecutive points on trajectory P^1 and P^2 (*i.e.*, $P^1_i, P^1_{i+1}, P^2_i, P^2_{i+1}$) to build a quadrilateral, resulting in $N-1$ quadrilaterals. To ensure collecting all the objects, the centers of all circles O must be covered by these quadrilaterals. Moreover, to prevent the path from enclosing any obstacles inside, these quadrilaterals must not overlap with any obstacles.

III. Robust Trajectory Tracking Control

We adopt a decentralized framework to design the trajectory tracking controller for individual WMRs. Since the drag force from the tethered net and gathered objects are unknown in our proposed setup, the conventional model-based controller is not suitable, and a more advanced MRAC is implemented to improve the robustness of the trajectory tracking control.

A. Dynamics of Individual WMRs

The configuration of WMRs is defined by $q = [x, y, \phi]$, shown also in Fig. 2. Li *et al.* [29] describe its dynamics:

$$M(q)\ddot{q} + C(q, \dot{q})\dot{q} = B(q)\tau - A(q)^T\lambda, \tag{12}$$

where

$$M(q) = \begin{bmatrix} m & 0 & md\sin\phi \\ 0 & m & -md\cos\phi \\ md\sin\phi & -md\cos\phi & J \end{bmatrix}, \tag{13}$$

$$C(q, \dot{q}) = \begin{bmatrix} 0 & 0 & md\dot{\phi}\cos\phi \\ 0 & 0 & -md\dot{\phi}\sin\phi \\ 0 & 0 & 0 \end{bmatrix}, \tag{14}$$

$$B(q) = \frac{1}{r}\begin{bmatrix} \cos\phi & \cos\phi \\ \sin\phi & \sin\phi \\ R & -R \end{bmatrix}, \tag{15}$$

$$A(q) = \begin{bmatrix} -\sin\phi & \cos\phi & -d \end{bmatrix}, \tag{16}$$

$$\lambda = -m(\dot{x}\cos\phi + \dot{y}\sin\phi)\dot{\phi}, \tag{17}$$

where m is the WMR's mass, J its rotational inertia, $2R$ the distance between two driving wheels, r the radius of each wheel, d the distance from the coordinate origin P_0 to the CoM P_c, $M(q)$ the inertia matrix, $C(q, \dot{q})$ the Coriolis and Centrifugal force matrix, $B(q)$ the input transformation matrix, τ the torque vector for two wheels, $A(q)$ matrix associated with the non-holonomic constraints (*i.e.*, $A(q)\dot{q} = 0$), and λ the vector of constraint forces. Selecting $S(q)$ as a basis of $A(q)$ nullspace (*i.e.*, $S(q)^T A(q)^T = 0$),

$$S(q) = \begin{bmatrix} \cos\phi & -d\sin\phi \\ \sin\phi & d\cos\phi \\ 0 & 1 \end{bmatrix}, \tag{18}$$

we can rewrite the WMR's kinematic equation with the velocity vector,

$$\dot{q} = S(q)v, \tag{19}$$

where $v = [\nu, \omega]^T$, and ν and ω are the WMRs' linear and angular velocity. Taking the derivative of Eq. (19), we have

$$\ddot{q} = \dot{S}(q)v + S(q)\dot{v}. \tag{20}$$

Substituting Eqs. (19) and (20) into Eq. (12) and multiplying S^T at each side, we have

$$\bar{M}\dot{v} + \bar{C}v = \bar{\tau}, \tag{21}$$

where $\bar{M} = S(q)^T M(q) S(q)$, $\bar{\tau} = \bar{B}\tau$, $\bar{B} = S(q)^T B(q)$, and $\bar{C} = S(q)M(q)\dot{S}(q) + S(q)^T C(q, \dot{q})S(q)$.

B. Model-Based Control of Individual WMRs

We design a conventional model-based controller based on Eq. (21) as a baseline,

$$\tau = \bar{B}^{\dagger}(\bar{M}\dot{v}^d + \bar{C}v^d), \tag{22}$$

where v^d is the desired velocity vector, designed to track the reference trajectory [29]:

$$v^d = \begin{bmatrix} \nu^d \\ \omega^d \end{bmatrix} = \begin{bmatrix} \nu^r \cos e_\phi + k_1(e_x + d(1 - \cos e_\phi)) \\ \omega^r + k_2\nu^r(e_y - d\sin e_\phi + k_3\nu^r \sin e_\phi) \end{bmatrix}, \tag{23}$$

where ν^r and ω^r are reference linear and angular velocity, k_1, k_2, and k_3 are positive parameters, and e_x, e_y, and e_ϕ are errors between the reference trajectory and the real trajectory in x, y, and ϕ, respectively [29],

$$e_x = x^r - x,\ e_y = y^r - y,\ e_\phi = \phi^r - \phi. \tag{24}$$

Although this controller has proven to work well on WMRs given accurate physical parameters, it fails in our setting because the tethered net will collect multiple objects with unknown physic parameters (mass, inertia, *etc.*). As such, we further design an adaptive control law; see the next section.

C. Adaptive Control with Unknown Payload

Since MRAC laws guarantee the asymptotic convergence of trajectory tracking error in the presence of parametric and matched uncertainties [19], we implement MRAC on WMRs to improve its robustness under unknown payload.

Specifically, we rewrite the matrices in Eq. (21) with unknown dynamics,

$$\begin{aligned}\bar{M} &= \bar{M}_k + \bar{M}_u^* = (\bar{M}_k - I) + (I + \bar{M}_u^*)\\ &= (\bar{M}_k - I) + \bar{M}_u,\\ \bar{C} &= \bar{C}_k + \bar{C}_u,\end{aligned} \tag{25}$$

where k and u denote the known and unknown dynamics, respectively. Combining Eq. (25) with Eq. (21), we have

$$\dot{X}(t) = A_r X(t) + B_r u(t), \tag{26}$$

where $X = v$, $A_r = -\bar{M}_u^{-1}\bar{C}_u$, and $B_r = \bar{M}_u^{-1}$. The input $\bar{\tau}$ can be recovered by

$$\bar{\tau} = u + (\bar{M}_k - I)\dot{v}(t) + \bar{C}_k v(t), \tag{27}$$

and the reference model is given as

$$\dot{X}_m(t) = A_m X_m(t) + B_m u_m(t), \tag{28}$$

where $X_m = v^d$, $A_m = -K$, K is a Hurwitz matrix, and $B_m = I$. The reference input u_m can be calculated by

$$u_m = B_m^{-1}(\dot{X}_m - A_m X_m) = \dot{v}^d + Kv^d. \tag{29}$$

The adaptive law is designed as

$$\begin{aligned}u &= \bar{u}_a + \bar{u}_k,\\ \bar{u}_k &= -KX + u_m,\\ \bar{u}_a &= -\Delta_X X + \Delta_m u_m,\end{aligned} \tag{30}$$

where $\bar{u}_k$ and $\bar{u}_a$ are the linear and adaptive feedback component, respectively. $\dot{\Delta}_X$ and $\dot{\Delta}_m$ can be calculated with adaptive gains and state errors; please refer to Canigur *et al.* [21] for more details. Of note, the motor torque saturation and the adaptive gains of MRAC jointly determine the maximum payload while the stability of tracking controller is still maintained. Larger adaptive gains can increase the response speed but may lead to oscillations and higher overshoot [30].

IV. Simulation

This section evaluates our cooperative planning framework in a simulation environment based on Gazebo, a 3D dynamic environment simulator. Our results demonstrate that (i) the proposed framework produces optimal trajectories for the tethered robots, and (ii) our U-shape cost function design effectively maintains the tethered net during the tasks.

A. Setup

For the tethered robot platform, we utilize two TurtleBot3 Waffle Pi robots and tether them with a flexible "net" by connecting several 0.1-meter-long thin cuboid links with passive revolute joints; the length of the net can be easily modified by inserting or removing cuboid links. With such a design, the tethered net would deform in accord to gathered objects' weights, and drag forces could be introduced to robots in an unspecified direction, crucial in evaluating our MRAC implementation. To enable torque command to the robots in simulation, we use *JointEffortController* in *ros_control* to command desired torques to TurtleBot3's wheels instead of using the built-in controller with velocity control only.

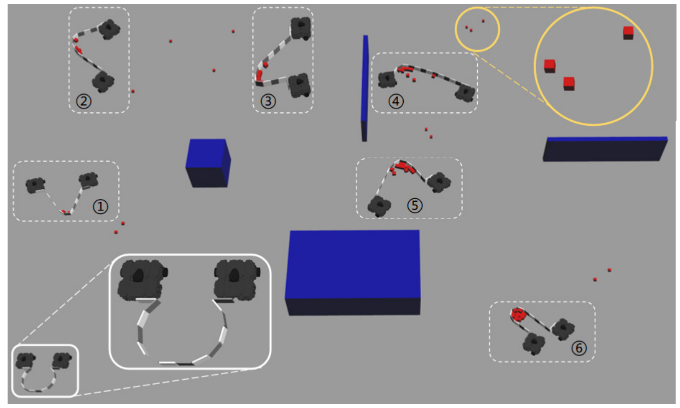

Fig. 4: **The simulation environment.** The tethered robot duo is tasked to gather 13 objects (red cubes), navigating from the bottom left to the bottom right. The dashed boxes depict some key moments when the duo gathers objects with the flexible net.

Fig. 4 illustrates the simulated environment with several keyframes of a task performance. The tethered robot duo starts from the bottom left to gather red movable cubes while avoiding blue obstacles at various locations. Table I tabulates some essential physical and software properties of the simulation setup. We set the parameters involved in the trajectory planning as following: $l = 0.3\ m$, $N_{\text{total}} = 8$, $t_1 = 300$, $t_2 = 10$, $K_1 = K_2 = K_3 = 1e7$, $k_{d1} = 20$, $k_{d2} = 15$, $b_1 = b_2 = 110$, $b_3 = 1$, $a_1 = a_2 = a_3 = a_4 = 1$, $\Delta L_{\max} = 0.05\ m$, and $\Delta\phi_{\max} = 0.1\ rad$. We utilize the nonlinear optimization solver `fmincon` in Matlab to solve the optimal trajectory with the interior point method.

B. Trajectory Tracking

Fig. 5 shows the simulation results with various lengths of the tethered net $d_{\max}$. Given a configuration during the

TABLE I: Physical and Software Properties used in Simulation

Group	Parameter	Value
Robot	Mass m	$1.43\ kg$
	Moment J	$0.146\ kg \cdot m^2$
	R	$0.144\ m$
	r	$0.033\ m$
	d	$0.020\ m$
Net	Mass of each cuboid link	$2\ g$
	Size of each cuboid link $d \times w \times h$	$1 \times 10 \times 8\ cm^3$
	Damping of each cuboid joint	$1e-3$
	Friction of each cuboid joint	$\mu_1 = \mu_2 = 0.2$
Others	Mass of object cube m_i	$25\ g$
	Size of object cube	$5 \times 5 \times 5\ cm^3$
	Trajectory tracking controller rate	$100\ Hz$
	Motor torque controller rate	$500\ Hz$

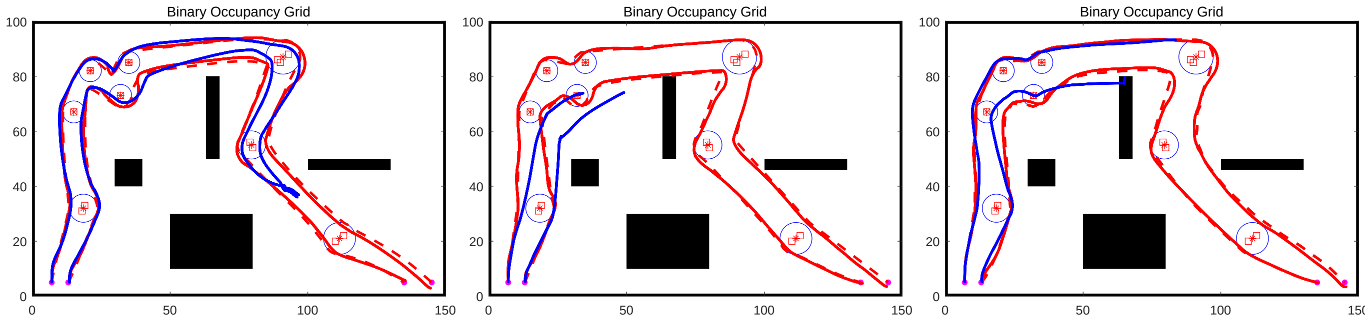

(a) Trajectory tracking $d_{\max} = 1.5\ m$ (b) Trajectory tracking $d_{\max} = 2.0\ m$ (c) Trajectory tracking $d_{\max} = 2.32\ m$

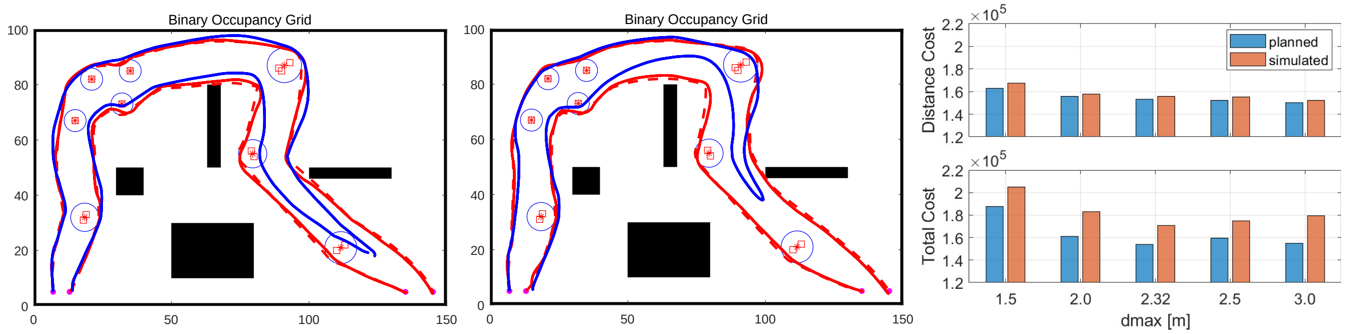

(d) Trajectory tracking $d_{\max} = 2.5\ m$ (e) Trajectory tracking $d_{\max} = 3.0\ m$ (f) Simulation cost and planing cost

Fig. 5: (a–e) **The schematic of the simulated environment constructed in Gazebo.** With various lengths of the tethered net, our cooperative planning framework produces reference trajectory (dashed red lines). Tracked trajectories by the proposed MRAC controller and conventional model-based controller are visualized in solid red and blue lines, respectively; the MRAC controller can robustly track trajectories, whereas the conventional controller constantly fails as the task progresses. (f) **Distance cost and total cost of the optimized trajectories in the planning and the simulated execution phases.** Our framework further produces the optimal $d_{\max} = 2.32\ m$ for a given configuration.

optimization, our framework can further estimate the optimal length of the tethered net in terms of defined cost function J_{total} by treating $d_{\max}$ as a variable in Algorithm 1. If $d_{\max}$ is already specified, Algorithm 1 can be easily modified by treating $d_{\max}$ as a constant instead of a variable. Among five cases with various maximum net lengths shown in Fig. 5, our framework estimates $d_{\max} = 2.32\ m$ is the optimal net length.

In these simulations, we implement both MRAC controller and the conventional model-based controller. Specifically, the MRAC controller can maintain the platform stability along the whole trajectory while successfully gathering and transporting all the objects to the endpoint. By contrast, the conventional model-based controller is unstable when more objects are collected, resulting in collisions between the two robots or between the robot and objects/obstacles.

For each of the above cases, the distance cost J_{dist} and total cost J_{total} are first obtained with recorded robot trajectory. Next, these costs are compared with planned costs; the results are shown in Fig. 5f. In particular, if we only care about J_{dist}, both $d_{\max} = 2.5\ m$ and $d_{\max} = 3.0\ m$ are better. However, it is difficult to maintain the shape of the tethered net under these two settings. As such, our optimization framework deems they are not the optimal solution. In comparison, although $d_{\max} = 2.32\ m$ results in a slightly higher J_{dist}, this length is considered as the optimal one due to the lowest J_{total}.

This simulation result demonstrates the tracking performance of the proposed MRAC controller to handle increasing payloads. It also suggests that a longer tether between robots does not necessarily correspond to better efficiency. This finding may impact prior arts wherein the length is not considered [4, 14] or is fixed [5, 6, 17, 18, 31].

C. Maintaining Net Shape

We design a U-shape cost function in Eq. (8) to penalize the tethered robot duo for being too close/far, so that the curvature of the net is indirectly controlled to embrace new objects and carry gathered objects. To demonstrate the efficacy of the U-shape design, we compare with two baseline cost functions:

- **No separation constraint included**. This strategy does not take separation distance into consideration [4]; referred to as Baseline 1 in Fig. 6.
- **Desired separation distance d_{rest} as hard constraint**. This strategy maintains the desired separation distance along the path [6, 17, 18, 31]; referred to as Baseline 2 in Fig. 6.

Figs. 6b, 6d and 6f quantitatively compare the distance cost of each cost design with various net lengths in three scenarios, and Figs. 6a, 6c and 6e show the corresponding reference trajectories produced by our framework using the 3 types of expansion cost designs with a specific net length in each scenario. Although Baseline 1 yields the shortest travel distance without including any constraint on separation distance, it may require unrealistic net length. Baseline 2 keeps a specified separation distance at all time, which may find no solution for a small $d_{\max}$ or cause unnecessarily long travel distance for a large $d_{\max}$. In comparison, the proposed U-shape cost function produces feasible solutions for various $d_{\max}$ while properly maintaining efficient travel distances.

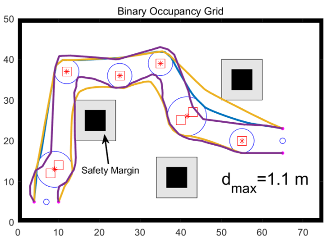

(a) Trajectory comparison

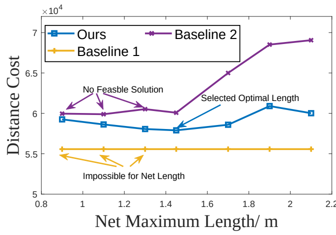

(b) Shape cost comparison

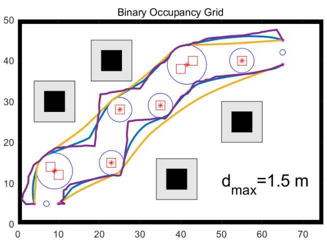

(c) Trajectory comparison

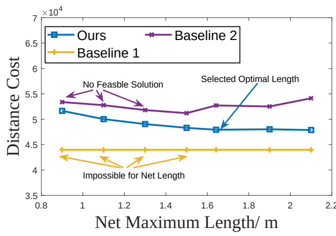

(d) Shape cost comparison

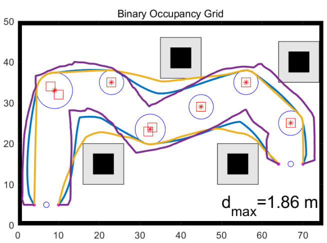

(e) Trajectory comparison

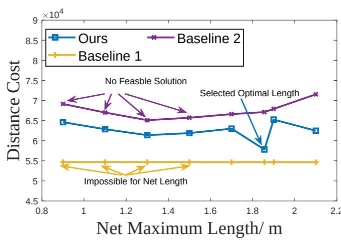

(f) Shape cost comparison

Fig. 6: Planned trajectories with various expansion cost function designs in three scenarios; each row corresponds to one scenario.

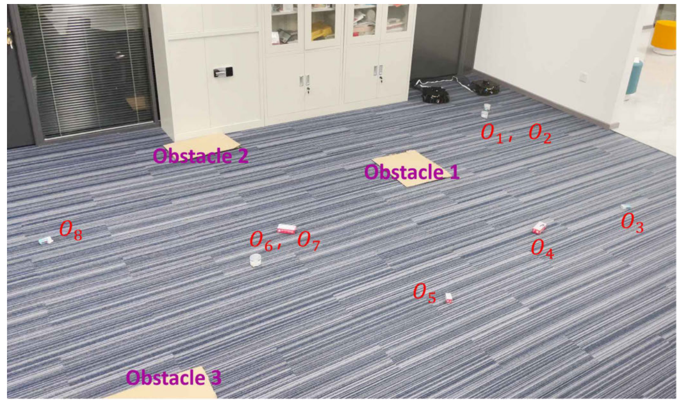

(a) **Experimental environment.** Eight objects are placed on the floor. The robot duo is tasked to gather them with a tethered net while avoiding obstacles during its navigation.

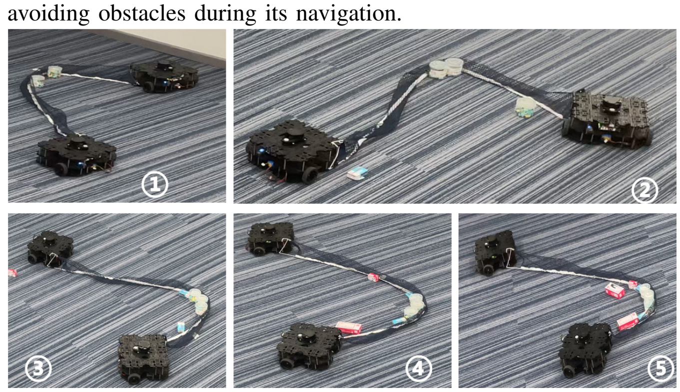

(b) Five keyframes of gathering objects captured with varying weights during the robot duo's task execution.

Fig. 7: Experiments with MRAC implementation in a robot duo in the physical environment.

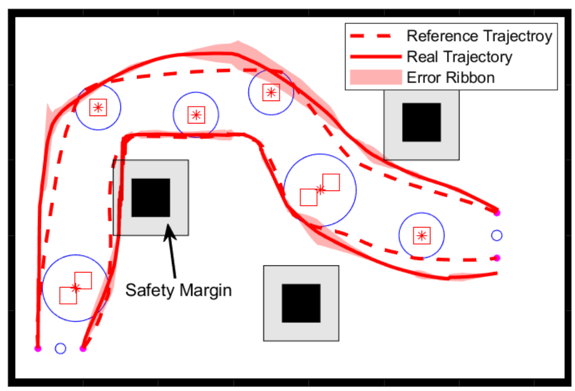

Fig. 8: **Reference and tracked trajectories of the tethered robot duo.** The red shadows indicate the variations of five executions.

V. Experiment

Section IV has evaluated the proposed cooperative planning framework and the MRAC controller design in simulation. This section further validates the proposed framework in the physical environment.

A. Setup

The setup of our proposed tethered robot duo is shown in Fig. 1b, wherein a net is connected to two TurtleBot3 Waffle Pi robots at each end. Each TurtleBot is equipped with a Raspberry Pi 3B+ running Robot Operating System (ROS), an OpenCR 1.0 board with an IMU module and a microprocessor for low-level motor control, an LDS-01 Lidar for localization, and two Dynamixel XM430 motors with a maximum torque of $3\ N{\cdot}m$ for wheel actuation. The path planning component runs on a desktop (AMD Ryzen9 5950X CPU, 64.00 GB RAM) and takes an average of $180.3\ s$ to produce the optimal trajectory with $N = 200$ in Algorithm 1.

To enable torque command, we modify the built-in low-level controller on OpenCR board designed to take velocity command inputs, such that it receives torque command inputs. The Gmapping Simultaneous Localization and Mapping (SLAM) algorithm is utilized to localize the WMRs in experiment and outputs q and v as feedback. Fig. 7a shows the experimental environment, a replication of the simulated environment presented in Fig. 6a; eight objects are placed on the floor with various weights ranging from $15\ g$ to $50\ g$.

B. Results

The net length used in our experiment is $1.45\ m$, the optimal length estimated by our cooperative path planner according to this specific environment configuration. Fig. 8 plots the reference and actual trajectories with error ribbon aggregated from five trials. Together with the simulation results, our experiments have demonstrated (i) the implemented MRAC controller robustly tracks the planned trajectories, and (ii) the tethered robot duo, using the proposed cooperative planning framework, successfully gathers all the objects along the path and carries them to the end position.

VI. Conclusion

This paper investigated an interesting task of gathering and transporting scattered objects with a tethered robot duo. We addressed it by proposing a two-stage cooperative planning framework based on trajectory optimization and implementing it with MRAC. In planning, we designed a U-shape cost function and incorporated other constraints to produce trajectories, capable of indirectly maintaining the flexible net's shape w.r.t. the distance between two robots. In the implementation, we demonstrated that MRAC could robustly handle the increased payload with unknown dynamics as more objects were carried. As an extra feature, our planning framework can also estimate the most efficient length given an environment configuration, which led to a crucial extension to existing work in tethered robots that assumed an infinite or fixed tether length. Both the simulation and experiment results have demonstrated the efficacy of the proposed framework and the necessity of MRAC implementation. In future work, we plan to (i) extend this framework to tethered Unmanned Surface Vehicle (USV) and drones for collaborative tasks, (ii) incorporate a perception module when the environment configuration is not fully available, and (iii) enable effective re-planning for the robot duo to account for new observations.

VII. Acknowledgement

The authors would like to thank Dr. Bo Dai, Mr. Ziyuan Jiao, Mr. Aoyang Qin, and Ms. Zhen Chen at BIGAI for their constructive discussions and help on experiments and figures.

References

[1] M. M. Gulzar, S. T. H. Rizvi, M. Y. Javed, U. Munir, and H. Asif, "Multi-agent cooperative control consensus: A comparative review," *Electronics*, vol. 7, no. 2, p. 22, 2018.

[2] A. Yamashita, T. Arai, J. Ota, and H. Asama, "Motion planning of multiple mobile robots for cooperative manipulation and transportation," *IEEE Transactions on Robotics and Automation*, vol. 19, no. 2, pp. 223–237, 2003.

[3] S. Heshmati-Alamdari, G. C. Karras, and K. J. Kyriakopoulos, "A predictive control approach for cooperative transportation by multiple underwater vehicle manipulator systems," *IEEE Transactions on Control Systems Technology*, 2021.

[4] S. Bhattacharya, S. Kim, H. Heidarsson, G. S. Sukhatme, and V. Kumar, "A topological approach to using cables to separate and manipulate sets of objects," *International Journal of Robotics Research (IJRR)*, vol. 34, no. 6, pp. 799–815, 2015.

[5] R. H. Teshnizi and D. A. Shell, "Motion planning for a pair of tethered robots," *Autonomous Robots*, pp. 1–15, 2021.

[6] D. S. D'antonio, G. A. Cardona, and D. Saldaña, "The catenary robot: Design and control of a cable propelled by two quadrotors," *IEEE Robotics and Automation Letters (RA-L)*, vol. 6, no. 2, pp. 3857–3863, 2021.

[7] G. A. Cardona, D. S. D'Antonio, C.-I. Vasile, and D. Saldana, "Non-prehensile manipulation of cuboid objects using a catenary robot," in *Proceedings of International Conference on Intelligent Robots and Systems (IROS)*, 2021.

[8] T. Furukawa, F. Bourgault, B. Lavis, and H. F. Durrant-Whyte, "Recursive bayesian search-and-tracking using coordinated uavs for lost targets," in *Proceedings of International Conference on Robotics and Automation (ICRA)*, 2006.

[9] I. I. Hussein and D. M. Stipanovic, "Effective coverage control for mobile sensor networks with guaranteed collision avoidance," *IEEE Transactions on Control Systems Technology*, vol. 15, no. 4, pp. 642–657, 2007.

[10] L. Yan, T. Stouraitis, and S. Vijayakumar, "Decentralized ability-aware adaptive control for multi-robot collaborative manipulation," *IEEE Robotics and Automation Letters (RA-L)*, vol. 6, no. 2, pp. 2311–2318, 2021.

[11] R. Ritz, M. W. Müller, M. Hehn, and R. D'Andrea, "Cooperative quadrocopter ball throwing and catching," in *Proceedings of International Conference on Intelligent Robots and Systems (IROS)*, 2012.

[12] X. Zhang, F. Zhang, P. Huang, J. Gao, H. Yu, C. Pei, and Y. Zhang, "Self-triggered based coordinate control with low communication for tethered multi-uav collaborative transportation," *IEEE Robotics and Automation Letters (RA-L)*, vol. 6, no. 2, pp. 1559–1566, 2021.

[13] J. Fink, N. Michael, S. Kim, and V. Kumar, "Planning and control for cooperative manipulation and transportation with aerial robots," *International Journal of Robotics Research (IJRR)*, vol. 30, no. 3, pp. 324–334, 2011.

[14] S. Kim, S. Bhattacharya, H. K. Heidarsson, G. S. Sukhatme, and V. Kumar, "A topological approach to using cables to separate and manipulate sets of objects.," in *Proceedings of Robotics: Science and Systems (RSS)*, 2013.

[15] P. Mitrano, D. McConachie, and D. Berenson, "Learning where to trust unreliable models in an unstructured world for deformable object manipulation," *Science Robotics*, vol. 6, no. 54, 2021.

[16] J. Alonso-Mora, R. Knepper, R. Siegwart, and D. Rus, "Local motion planning for collaborative multi-robot manipulation of deformable objects," in *Proceedings of International Conference on Robotics and Automation (ICRA)*, 2015.

[17] M. Laranjeira, C. Dune, and V. Hugel, "Catenary-based visual servoing for tethered robots," in *Proceedings of International Conference on Robotics and Automation (ICRA)*, 2017.

[18] M. Laranjeira, C. Dune, and V. Hugel, "Catenary-based visual servoing for tether shape control between underwater vehicles," *Ocean Engineering*, vol. 200, p. 107018, 2020.

[19] E. Lavretsky and K. A. Wise, "Robust adaptive control," in *Robust and adaptive control*, pp. 317–353, Springer, 2013.

[20] R. B. Anderson, J. A. Marshall, and A. L'Afflitto, "Constrained robust model reference adaptive control of a tilt-rotor quadcopter pulling an unmodeled cart," *IEEE Transactions on Aerospace and Electronic Systems*, vol. 57, no. 1, pp. 39–54, 2020.

[21] E. Canigur and M. Ozkan, "Model reference adaptive control of a nonholonomic wheeled mobile robot for trajectory tracking," in *International Symposium on Innovations in Intelligent Systems and Applications*, 2012.

[22] J. Petereit, T. Emter, C. W. Frey, T. Kopfstedt, and A. Beutel, "Application of hybrid a* to an autonomous mobile robot for path planning in unstructured outdoor environments," in *German Conference on Robotics*, 2012.

[23] J. D. Gammell, S. S. Srinivasa, and T. D. Barfoot, "Informed rrt*: Optimal sampling-based path planning focused via direct sampling of an admissible ellipsoidal heuristic," in *Proceedings of International Conference on Intelligent Robots and Systems (IROS)*, 2014.

[24] C. L. Byrne, "Lecture notes on iterative optimization algorithms," *Department of Mathematical Sciences, University of Massachusetts Lowell*, 2014.

[25] C. T. Kelley, *Iterative methods for optimization*. SIAM, 1999.

[26] M. C. Lee and M. G. Park, "Artificial potential field based path planning for mobile robots using a virtual obstacle concept," in *International Conference on Advanced Intelligent Mechatronics*, 2003.

[27] M. Ryll, H. H. Bülthoff, and P. R. Giordano, "A novel overactuated quadrotor unmanned aerial vehicle: Modeling, control, and experimental validation," *IEEE Transactions on Control Systems Technology*, vol. 23, no. 2, pp. 540–556, 2014.

[28] M. Kalakrishnan, S. Chitta, E. Theodorou, P. Pastor, and S. Schaal, "Stomp: Stochastic trajectory optimization for motion planning," in *Proceedings of International Conference on Robotics and Automation (ICRA)*, 2011.

[29] L. Li, T. Wang, Y. Xia, and N. Zhou, "Trajectory tracking control for wheeled mobile robots based on nonlinear disturbance observer with extended kalman filter," *Journal of the Franklin Institute*, vol. 357, no. 13, pp. 8491–8507, 2020.

[30] J. E. Stellet, "Influence of adaptation gain and reference model parameters on system performance for model reference adaptive control," *World Academy of science, engineering and technology*, vol. 60, pp. 1768–1773, 2011.

[31] K. A. Talke, M. De Oliveira, and T. Bewley, "Catenary tether shape analysis for a uav-usv team," in *Proceedings of International Conference on Intelligent Robots and Systems (IROS)*, 2018.